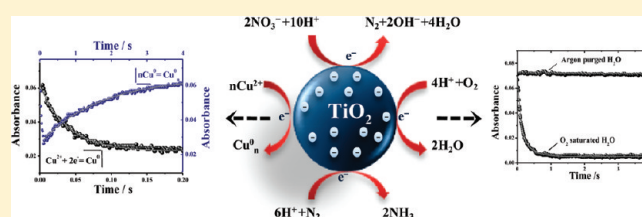


Kinetic and Mechanistic Investigations of Multielectron Transfer Reactions Induced by Stored Electrons in TiO₂ Nanoparticles: A Stopped Flow Study

Hanan H. Mohamed,^{†,‡} Cecilia B. Mendive,^{†,§} Ralf Dillert,[†] and Detlef W. Bahnemann^{*,†}[†]Institut für Technische Chemie, Leibniz Universität Hannover, Callinstrasse 3, D-30167 Hannover, Germany[‡]Chemistry Department, Faculty of Science, Helwan University, Ain Helwan, Cairo, Egypt[§]Departamento de Química, Facultad de Ciencias Exactas y Naturales, Universidad Nacional de Mar del Plata, Dean Funes 3350, 7600 Mar del Plata, Argentina

ABSTRACT: The kinetics and the mechanism of various multielectron transfer reactions initiated by stored electrons in TiO₂ nanoparticles have been investigated employing the stopped flow technique. Moreover, the optical properties of the stored electrons in the TiO₂ nanoparticles have been studied in detail following the UV (A) photolysis of deaerated aqueous suspensions of TiO₂ nanoparticles in the presence of methanol. The reduction of common electron acceptors that are often present in photocatalytic systems such as O₂, H₂O₂, and NO₃⁻ has been investigated. The experimental results clearly show that the stored electrons reduce O₂ and H₂O₂ to water by multielectron transfer processes. Moreover, NO₃⁻ is reduced via the transfer of eight electrons evincing the formation of ammonia. On the other hand, the reduction of toxic metal ions, such as Cu(II), has been studied mixing their respective anoxic aqueous solutions with those containing the electrons stored in the TiO₂ particles. A two-electron transfer is found to occur, indicating the reduction of the copper metal ion into its non toxic metallic form. Other metal ions, such as Zn(II) and Mn(II), could not be reduced by TiO₂ electrons, which is readily explained on the bases of their respective redox potentials. The underlying reaction mechanisms are discussed in detail.



INTRODUCTION

Photocatalytic applications employing UV irradiated TiO₂ nanoparticles for the decontamination of organic compounds as well as for the detoxification of hazardous metal ions in wastewater have become a mature field of study during the past decades.^{1,2} Upon bandgap excitation of semiconducting TiO₂ particles, electrons are promoted to their conduction band with the simultaneous generation of holes in the valence band, both of which will be consumed in the photocatalytic reactions. In the absence of suitable adsorbed hole scavengers and in the presence of molecular oxygen (i.e., an electron scavenger), the remaining holes oxidize surface water to produce adsorbed hydroxyl radicals, which can subsequently induce further oxidation reactions. However, in the presence of an adsorbed hole scavenger such as methanol and in the absence of molecular oxygen the fate of the photogenerated electrons is still not clear. Bahnemann et al.³ reported that excess electrons are trapped close to the surface of colloidal TiO₂ particles forming Ti³⁺, which is characterized by broad absorption spectra with $\lambda_{\text{max}} = 650$ nm. O'Regan et al.⁴ observed near-infrared absorbance spectra when TiO₂ membranes were biased at a negative potential. The authors attributed these absorbance spectra to free conduction band electrons with only a small fraction of the electrons being trapped at surface sites. Boschloo and Fitzmaurice⁵ reported that the optical absorption of trapped electrons produced in

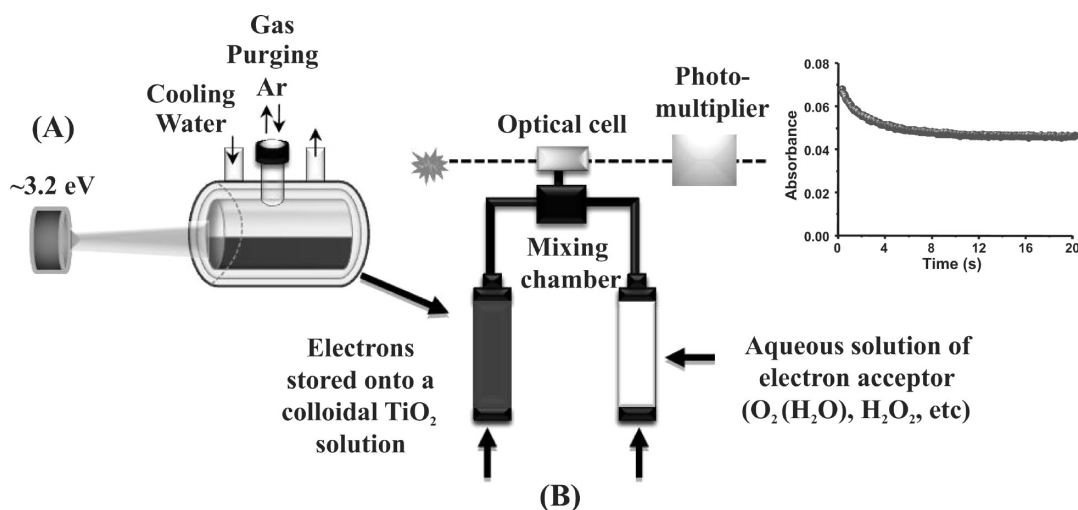
nanocrystalline TiO₂ layers under negative applied potential is strongest at 400 nm and gradually decreases to zero at 600 nm, which is superimposed with the visible absorption spectrum of conduction band electrons that is observed when applying a more negative potential. The authors determined the extinction coefficient of an electron trapped in a surface state to be $1900 \text{ M}^{-1} \text{ cm}^{-1}$ at $\lambda_{\text{max}} = 400$ nm, more than three times higher than that of a conduction band electron at the same wavelength.

A fundamental understanding of the dynamics of the charge carrier transfer at TiO₂ nanoparticles is of crucial importance for the understanding and industrialization of photocatalytic reactions as well as for the rational design of photocatalytic systems. During the last decades, much effort was devoted to the study of the kinetics and the mechanistic details of the interfacial electron transfer processes at the TiO₂/water interface using the laser flash photolysis technique. Grätzel and co-workers⁶ dealt with the transfer of electron and hole from the conduction and valence band of ultrafine TiO₂ and CdS particles to reactants in solution. Bahnemann et al.⁷ investigated the kinetics and mechanistic details of the processes occurring upon band gap irradiation in transparent suspensions of nanosized TiO₂ particles in the absence as well as in the presence of electron and hole scavengers. Recently, Gao et al.⁸ analyzed the kinetics of the

Received: September 19, 2010

Revised: January 3, 2011

Published: March 02, 2011

Scheme 1. Schematic Illustration of (A) the Method Employed to Store Electrons in TiO₂ Nanoparticles and (B) the Stopped Flow Experiment for the Multielectron Transfer Reactions

reactions of excess electrons in TiO₂ produced by radiolysis employing steady state and pulse radiolysis techniques.

The present work reports the results of an ongoing study concerning the kinetics and mechanism of a variety of reactions of stored electrons in TiO₂ nanoparticles employing the stopped flow technique. The basic concept of this work is rather straightforward, the electrons are generated on the TiO₂ nanoparticles by UV illumination in the presence of a hole scavenger, stored on them in the absence of molecular oxygen and subsequently used for the reduction of various oxidants such as O₂, H₂O₂, and NO₃⁻. The reduction of Cu²⁺ has also been studied following not only the decay of the transient absorbance of the trapped electrons but also by the detection of the respective surface plasmon absorbance band of the resulting metal clusters.

EXPERIMENTAL SECTION

Materials. All chemicals were of the highest purity available and were used as received without further purification: TiCl₄ (99.9%), methanol (99.99%), NaNO₃ (99.995%), and H₂O₂ (30%). They were all purchased from Sigma-Aldrich Company. All metal salts were chlorides (CuCl₂, MnCl₂, ZnCl₂). Nessler's reagent was used as received. All solutions were prepared with deionized water from a SARTORIUS ARIUM 611 apparatus (resistivity = 18.2 Ω cm).

Preparation of TiO₂ Nanoparticles. For transient absorption measurements in the stopped flow studies it is important that the light scattering of the particles is negligible, which can be achieved using transparent colloidal suspensions of small particle size. The transparent TiO₂ nanoparticles (2–3 nm particle size) have been prepared following the recipe reported by Kormann et al.⁹ A 3 mL quantity of titanium tetrachloride, TiCl₄, prechilled to -20 °C, was added slowly to 900 mL of vigorously stirred deionized water at 0 °C. After being continuously stirred for 1 h, the resulting transparent colloidal suspension was dialyzed using deionized water to bring the pH to 2.3. The colloid was dried by vacuum evaporation at 20 mbar at 27 °C. Off-white shining crystals were obtained, which can be resuspended in pure water to obtain perfectly transparent colloidal TiO₂ suspensions.

Analytical Methods. The UV–vis spectra over a range of 200–800 nm were recorded employing a Varian Cary 100 Scan UV–vis system. Transmission electron microscopy (TEM) was conducted at 200 kV with a JEOL JEM-2100F-UHR field-emission instrument equipped with a Gatan GIF 2001 energy filter and a 1k-CCD camera. X-ray diffraction (XRD) data were acquired on a Bruker AXS D4 Endeavor X diffractometer using Cu Kα_{1/2}, λα₁ = 154.060 pm, λα₂ = 154.439 pm radiation. The concentration of dissolved oxygen in water was determined using a Microprocessor Oximeter oxi 2000 in combination with a Trioximatic EO 200 electrode. The Gas Chromatographic (GC) measurements were carried out using a Shimadzu GC (Shimadzu 8A) equipped with a molecular sieve 5 Å packed column for analysis of inorganic gases. Argon was used as the carrier gas and a thermal conductivity detector (TCD) was employed for the gas detection.

Storing of Electrons on TiO₂ Nanoparticles. The electrons were stored on the TiO₂ nanoparticles by illuminating a deaerated (Argon purged) freshly prepared transparent colloidal suspension of 3 g/L TiO₂ (3.8 × 10⁻² M in terms of TiO₂ molecules) for 4 h in the presence of 0.02 M methanol as a hole scavenger. The UV (A) illumination was performed using a high-pressure Xe-lamp (OSRAM HBO-500W) placed inside a quartz jacket and equipped with a cooling tube (cf. Scheme 1 (A)). The employed UV (A) light intensity was 2.6 × 10⁻³ J cm⁻² s⁻¹.

Determination of the Extinction Coefficient of the Electrons Stored on TiO₂ Nanoparticles. The extinction coefficient of the stored electrons in TiO₂ at 600 nm has been determined through the titration of the stored electrons with benzoquinone (BQ) in the strict absence of molecular oxygen. The stored electron absorbance at 600 nm decreases linearly with increasing benzoquinone concentration. The extinction coefficient of the stored TiO₂ electrons, that is, ε_{600nm} = 600 M⁻¹ cm⁻¹, has been obtained from the slope according to the stoichiometry of the reaction. This value agrees rather well with the values of 470 M⁻¹ cm⁻¹ and 800 M⁻¹ cm⁻¹ determined in acidic¹³ and alkaline¹⁴ solutions, respectively.

Stopped Flow Investigations. Stopped flow experiments were performed using a SX.17MV-R Rapid Mixing Spectrophotometer (Applied Photophysics, United Kingdom) working in the UV–vis range (from 200–700 nm) with 0.2 cm optical

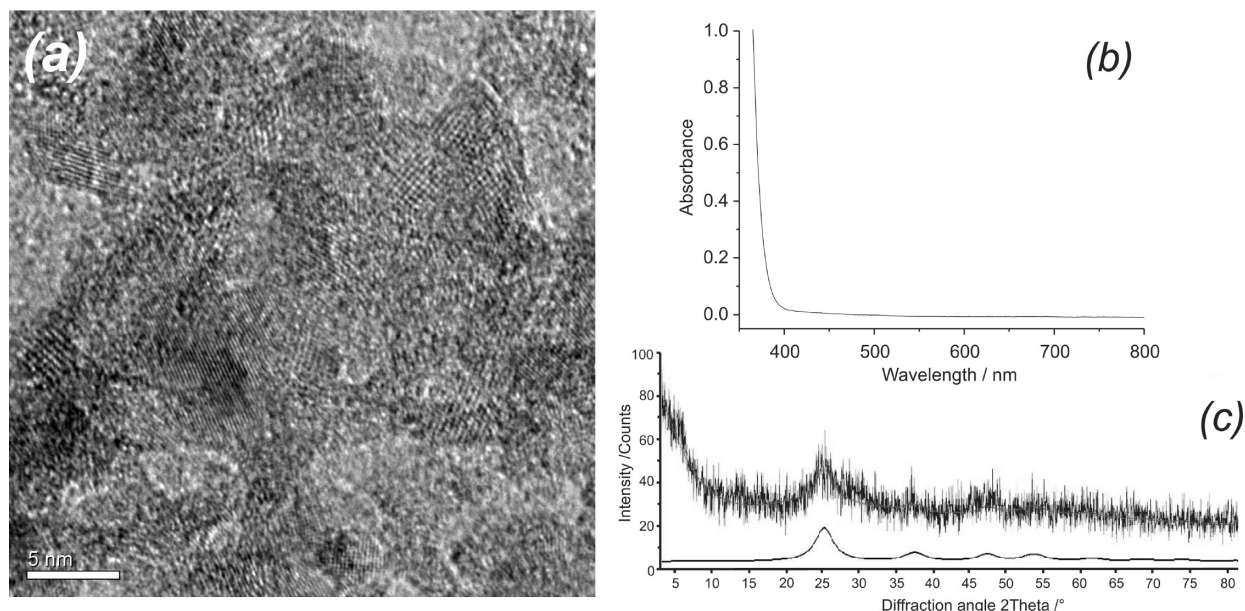


Figure 1. (a) HRTEM micrograph of the as-prepared TiO_2 , (b) UV–vis absorbance of an aqueous suspension of the as-prepared TiO_2 nanoparticles (4 g/L), and (c) XRD pattern of the as-prepared TiO_2 (thick line) and pure anatase (thin line).

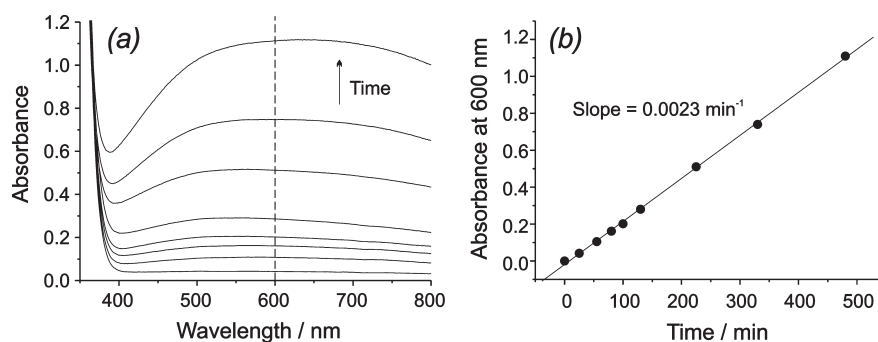


Figure 2. (a) Build up of the TiO_2 electron spectrum recorded at different periods of UV irradiation of a 3.8×10^{-2} M deaerated aqueous TiO_2 suspension in the presence of 0.02 M methanol at pH 2.3. (b) Absorbance at 600 nm as a function of the employed irradiation time. Reprinted with permission from *J. Photochem. Photobiol. A* **2011**, *217*, 271–274. Copyright 2010 Elsevier B.V.

path and 1 ms dead time. In a typical stopped flow experiment (cf. Scheme 1B), the suspension of the nanosized TiO_2 particles loaded with electrons was filled in one of the stopped flow syringes and an aqueous solution of the electron acceptor (metal ions, O_2 (H_2O), H_2O_2 , N_2 (H_2O), etc.) was filled into the other syringe. The solutions were injected into a mixing chamber (1:1 v/v), and the resulting reactant mixture reached the optical cell where the change in absorbance with time was measured. The kinetics of the electron transfer reactions was studied by following the decay of the absorbance of the TiO_2 electrons at 600 nm or the build-up of the absorption signals of the products, for example, the plasmonic bands of nanosized copper metal particles with time.

RESULTS AND DISCUSSION

Characterization of TiO_2 Nanoparticles. The absorption spectrum of 4 g/L TiO_2 nanoparticles resuspended in pure water is shown in Figure 1b. The absence of any light absorption above 400 nm evinces the presence of very small, that is,

non-light-scattering, particles. Due to the band gap energy of TiO_2 ($E_g = 3.2$ V for anatase),¹⁰ the absorption rises rapidly at wavelengths shorter than 390 nm. The crystalline character of the nanoparticles was investigated by XRD (cf. Figure 1c). The samples exhibit a broad diffraction pattern characteristic of the crystal phase of pure anatase of 3 nm particle size (as calculated from the XRD line broadening). The size of the TiO_2 particles was also determined using TEM measurements to be 2–3 nm, which is consistent with the XRD measurements (cf. Figure 1a).

Storing of Electrons on TiO_2 Nanoparticles. The UV (A) photolysis of a system containing TiO_2 (3.8×10^{-2} M) and methanol as hole scavenger in the absence of molecular oxygen results in the formation of a transparent blue suspension, indicating the generation of the stored electrons in the TiO_2 particles. Figure 2 shows the absorption spectra of the aqueous TiO_2 suspension observed after different UV irradiation periods. The blue coloration is characterized by a broad absorption band in the visible region with a maximum observed after 25 min of illumination and extending approximately from 510 to 700 nm.

In comparison to other works,¹³ such a maximum is not observed in systems where the electrons are first produced by γ irradiation in the solvent of TiO₂ suspensions and then transferred to the conduction band of the semiconductor (Figure 4 in ref 13). Although those spectra do not show a clear maximum, they remain approximately constant above 700 nm. We suggest that the spectral differences between Figure 2 and Figure 4 in ref 13 evince the two different methods employed for the production of stored electrons, that is, band gap excitation of the semiconductor to directly produce electrons in the conduction band (this work) and the indirect production of stored electrons employed in ref 13.

The photonic efficiency ζ of the storing of the TiO₂ electrons is calculated from the ratio of the rate of the buildup of the stored electrons (R) and the incident photon flux (J_0):¹¹

$$\zeta(\%) = \frac{R \cdot V}{J_0 \cdot A} \cdot 100$$

with

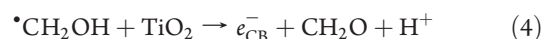
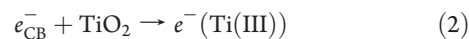
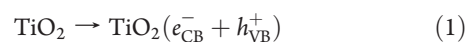
$$J_0 = \frac{I \cdot \lambda}{N_A \cdot h \cdot c}$$

I is the light intensity ($2.6 \times 10^{-3} \text{ J s}^{-1} \text{ cm}^{-2}$), which was calculated based on the UV light meter measurement, λ is the wavelength at the maximum emission (350 nm), N_A is Avogadro's number, h is Planck's constant, c is the light velocity, V is the volume ($6 \times 10^{-2} \text{ l}$), and A represents the irradiated surface area (12.56 cm^2). The average photonic efficiency measured under the above conditions was 3.8%.

The formation rate of the stored electrons (R) is calculated from the slope of the absorbance at 600 nm as a function of the illumination time (Figure 2b) to be $6 \times 10^{-8} \text{ M s}^{-1}$.

According to the mechanisms proposed in the literature,³ it is suggested that the TiO₂ electrons (e_t^-) are trapped as Ti(III) states. The shift of the absorption maximum of the stored TiO₂ electrons to longer wavelengths upon longer periods of illumination may be attributed to the storing of the excess electrons in the conduction band of TiO₂ after the available surface traps have been filled¹¹ or by the trapping of the electrons in the bulk rather than in surface traps, that is, assuming that bulk electron traps exhibit slightly red-shifted absorption spectra. The mechanism of electron storing can be summarized as follows (eqs 1–7a–d). Upon bandgap illumination electrons are promoted from the valence to the conduction band leaving holes behind in the valence band (eq 1). While the electrons are trapped at Ti(III) sites (eq 2) the valence band holes migrate to the surface of the particles where they react with the adsorbed methanol molecules producing α -hydroxyl methyl radicals (eq 3) that can directly inject electrons to the conduction band of the TiO₂ nanoparticle (eq 4). The process described by eqs 3 and 4 is known as current doubling.¹² The mobile and partially trapped holes can therefore recombine with excess electrons in the conduction band releasing heat (eq 5) and react with adsorbed chloride ions producing chlorine atoms (eq 6) and finally chlorine gas. This gas can either be produced by a termination reaction between two chlorine atoms (eq 7a) or involve the production of other radical intermediates with a high oxidative power such as $\text{Cl}_2^{\bullet-}$ ³³ (eqs 7b–7d). Indirect indications of a loss of chloride ions by conversion to chlorine are (i) the decrease in the chloride ion concentration measured after illumination and (ii) the blue coloration obtained by illuminating an aqueous TiO₂ suspension

in the absence of methanol, due to the stored TiO₂ electrons (data not shown).



33



33



33

Determination of the Number of Electrons per TiO₂ Nanoparticle. Assuming that the TiO₂ nanoparticles have a spherical shape, the volume of one TiO₂ particle with a diameter of 3 nm is calculated to be $1.41 \times 10^{-20} \text{ cm}^3$. Considering that the mass density of anatase TiO₂ is 3.894 g cm^{-3} , the average weight of one 3 nm TiO₂ nanoparticle is readily calculated to be $5.43 \times 10^{-20} \text{ g}$. In our system of 3 g/L TiO₂, the number of TiO₂ particles will consequently be 5.53×10^{19} particles/L.

The concentration of stored TiO₂ electrons was determined from the absorbance measurements (cf. Figure 2) using the extinction coefficient $\epsilon_{600 \text{ nm}} = 600 \text{ M}^{-1} \text{ cm}^{-1}$ obtained from the BQ titration experiments. The concentration of stored electrons ranges from 0.5×10^{-3} to $0.8 \times 10^{-3} \text{ M}$ ($30 - 48 \times 10^{19}$ electrons/L), corresponding to an average of about 6–9 electrons per TiO₂ particle.

Stopped Flow Investigations. As a blank experiment, the absorption spectrum of the stored electrons on TiO₂ was also measured using the stopped flow instrument. The blue colloidal suspension of the stored TiO₂ electrons at pH 2.3 was mixed with a deaerated aqueous HCl solution at the same pH in the stopped flow apparatus and the time evolution of the absorbance was recorded. Figure 3 shows the transient absorbance spectrum (380–660 nm) recorded 5 ms after mixing with 20 nm resolution; the typical absorption spectrum of stored TiO₂ electrons recorded with the spectrometer and prepared under the same conditions, that is, after 1:1 dilution of the stored TiO₂ electron suspension with deaerated aqueous HCl solution; and the last spectrum shown in Figure 2 normalized to the minimum at 390 nm to demonstrate that the shape of the spectrum is unchanged at the same wavelength range. The normalization was done to compare the spectrum shapes because they were recorded after different times of mixing the colloids with the solution at both equipments, that is, the stopped flow and the spectrometer. As depicted in Figure 2, a broad absorption maximum around 600 nm is as well observed in Figure 3. The inset of Figure 3 shows the transient absorption signal at 600

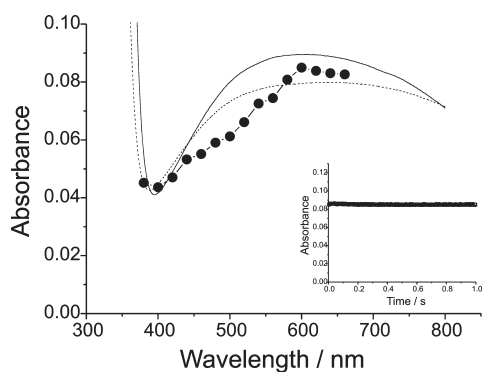


Figure 3. Transient absorption spectra measured after 5 ms of mixing a 3.8×10^{-2} M deaerated TiO_2 electron suspension at pH 2.3 (dots connected by straight lines to help the eye); steady state absorbance of the same system but scaled with a factor 5 due to the larger optical path of these type of measurements as compared to the small cuvette in the stopped flow equipment (solid line); and the last spectrum shown in Figure 2, which was normalized to the minimum at 390 nm (dotted line). Inset shows transient absorbance vs time signal after mixing of TiO_2 electrons with deaerated water at pH 2.3 (HCl). Reprinted with permission from *J. Photochem. Photobiol. A* **2011**, *217*, 271–274. Copyright 2010 Elsevier B.V.

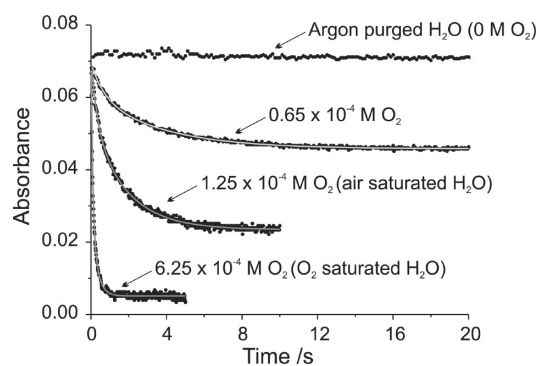


Figure 4. Time profiles of the decay of the $e^-_{\text{TiO}_2}$ absorbance at 600 nm ($[e^-_{\text{TiO}_2}] = 5.7 \times 10^{-4}$ M) upon mixing with different concentrations of dissolved O_2 saturated aqueous solutions at pH 2.3 (HCl). Solid gray lines over the points show the double exponential fits. Reprinted with permission from *J. Photochem. Photobiol. A* **2011**, *217*, 271–274. Copyright 2010 Elsevier B.V.

nm (mixing occurred at $t = 0$ s), which remains unchanged during the entire measurement time of 1 s.

1. *Reaction of $e^-_{\text{TiO}_2}$ with O_2 and H_2O_2 .* Figure 4 shows the transient absorption signals observed upon mixing aqueous stored TiO_2 electron suspensions ($[e^-_{\text{TiO}_2}] = 5.7 \times 10^{-4}$ M) at pH 2.3 with aqueous solutions containing different concentrations of O_2 (0.65×10^{-4} M, air-saturated (1.25×10^{-4} M), O_2 saturated (6.25×10^{-4} M), and argon saturated H_2O). A similar kinetic experiment for the reduction of hydrogen peroxide by the stored TiO_2 electrons was also performed. Figure 5 shows the transient absorption signals observed upon mixing the blue suspension of TiO_2 electrons ($[e^-_{\text{TiO}_2}] = 6.9 \times 10^{-4}$ M) at pH 2.3 with different concentrations of aqueous H_2O_2 solutions, that is, 1.56×10^{-4} , 3.12×10^{-4} , and 6.25×10^{-4} M. It is observed that in the argon flushed solution the absorbance signals decrease very slowly with a rate of 8.9×10^{-7} M s^{-1} , while in solutions containing dissolved O_2 or H_2O_2 the electron absorbance is

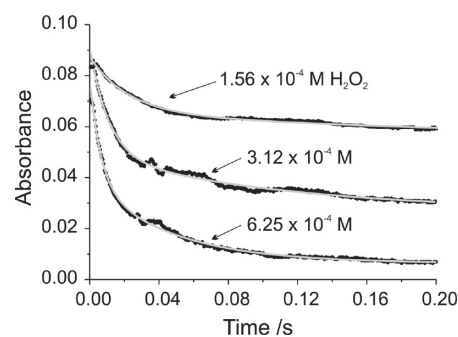


Figure 5. Time profiles of the decay of the $e^-_{\text{TiO}_2}$ absorbance at 600 nm ($[e^-_{\text{TiO}_2}] = 6.9 \times 10^{-4}$ M) upon mixing with Ar-purged H_2O_2 solutions at pH 2.3 (HCl). Reprinted with permission from *J. Photochem. Photobiol. A* **2011**, *217*, 271–274. Copyright 2010 Elsevier B.V.

fading rapidly, with the rate depending on the concentration of O_2 or H_2O_2 , respectively. The kinetic curves were analyzed according to a double exponential decay fitting. The observed first order rate constants were found to increase linearly with increasing the concentration of the electron acceptors (O_2 , H_2O_2) and the respective second order rate constants were obtained from the slope of the linear dependencies. The values of the resulting second order rate constants are summarized in Table 1.

The rate constant of the first initial decay ($k_{\text{I}}^{\text{obs}} = 2.0 \times 10^4 \text{ M}^{-1} \text{ s}^{-1}$) and that of the second decay ($k_{\text{II}}^{\text{obs}} = 5.7 \times 10^3 \text{ M}^{-1} \text{ s}^{-1}$) for the reaction of stored TiO_2 electrons with molecular oxygen were found to be similar to the values of the rate constants of the two slower processes k_{III} ($7.3 \pm 1.5 \times 10^3 \text{ M}^{-1} \text{ s}^{-1}$) and k_{IV} ($1.0 \pm 0.2 \times 10^3 \text{ M}^{-1} \text{ s}^{-1}$) reported by Gao et al.⁸ who studied the reaction of electrons formed by radiation chemical processes in small TiO_2 particles and who suggested that these slow processes are due to the reaction of excess TiO_2 electrons with molecular oxygen in the bulk.

Bahnemann et al.⁷ determined a reaction rate constant of $7.6 \times 10^7 \text{ M}^{-1} \text{ s}^{-1}$ for the reaction of trapped electrons produced by laser flash photolysis of platinumized TiO_2 nanoparticles with molecular oxygen producing the superoxide radical which is considerably higher than the present value. However, it is important to note that the experimental conditions differ considerably from those employed in the laser flash photolysis study and the present stopped flow experiments. While in the former just one electron/hole pair was generated at each TiO_2 nanoparticle during each single laser pulse, in the present study the TiO_2 particles contained between six and nine electrons each. Consequently, the observed differences can be attributed to multielectron transfer processes that are suggested to occur in the present system. Moreover, while the laser flash experiments were carried out employing a colloidal TiO_2 suspension in equilibrium with adsorbed and dissolved O_2 molecules, there is no molecular oxygen present on the surface of the TiO_2 particles here. Hence, all observed electron transfer processes clearly reflect reactions with dissolved electron acceptors. The present results can therefore be regarded as an experimental proof for the assumption of Gao et al.⁸ that the “slow processes” are indeed reflecting the electron transfer to dissolved O_2 molecules.

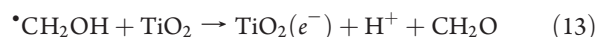
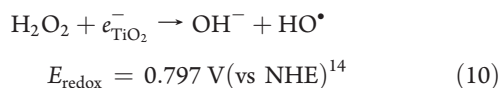
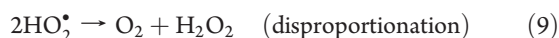
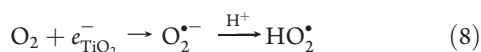
The rate constant of the first initial decay ($k_{\text{I}}^{\text{obs}} = 2.7 \times 10^5 \text{ M}^{-1} \text{ s}^{-1}$) and that of the second decay ($k_{\text{II}}^{\text{obs}} = 3.2 \times 10^4 \text{ M}^{-1} \text{ s}^{-1}$) for the reaction of the stored TiO_2 electrons with hydrogen peroxide are found to be in very good agreement with

Table 1. Summary of Rate Constants for the Reactions of Stored Electrons in TiO₂ Colloidal Particles with Different Electron Acceptors (Reprinted in Part with Permission from *J. Photochem. Photobiol. A* 2011, 217, 271–274. Copyright 2010 Elsevier B.V.)

electron acceptors	reaction pathway	$[e^-_{\text{TiO}_2}]/M$	number of transferred electrons	$k/M^{-1} s^{-1}$
O ₂	$e^-_{\text{TiO}_2} + \text{O}_2 + \text{H}^+ \rightarrow \text{HO}_2^\bullet$	5.7×10^{-4}	1.1	2×10^4
	$e^-_{\text{TiO}_2} + \text{HO}_2^\bullet + \text{H}^+ \rightarrow \text{H}_2\text{O}_2$		2	5.6×10^3
	$\text{H}_2\text{O}_2 + e^-_{\text{TiO}_2} \rightarrow \text{OH}^- + \text{OH}^\bullet$		total (3.1)	
	$2 e^-_{\text{TiO}_2} + \text{H}_2\text{O}_2 \rightarrow 2 \text{OH}^-$			
H ₂ O ₂	$\text{H}_2\text{O}_2 + e^-_{\text{TiO}_2} \rightarrow \text{OH}^- + \text{OH}^\bullet$	6.9×10^{-4}	1.1	2.7×10^5
	$2 e^-_{\text{TiO}_2} + \text{H}_2\text{O}_2 \rightarrow 2 \text{OH}^-$		0.5	3.2×10^4
	total (1.6)			
NO ₃ ⁻	$2\text{NO}_3^- + 12\text{H}^+ + 10e^-_{\text{TiO}_2} \rightarrow \text{N}_2 + 6 \text{H}_2\text{O}$ (17)	5.5×10^{-4}	4.6	1.7×10^4
	$\text{N}_2 + 4e^-_{\text{TiO}_2} + 5\text{H}^+ \rightarrow \text{N}_2\text{H}_5^+$ (18)		3.3	1.6×10^3
	$\text{N}_2\text{H}_5^+ + 2e^-_{\text{TiO}_2} + 3\text{H}^+ \rightarrow 2\text{NH}_4^+$ (19)		total (7.9)	
Cu ²⁺	$\text{Cu}^{2+} + 2e^-_{\text{TiO}_2} \rightarrow \text{Cu}^0$	5.4×10^{-4}	1.7	9.4×10^4
	$n\text{Cu}_0 \rightarrow \text{Cu}_n^0$			$k_1 = 0.6 \text{ s}^{-1}$

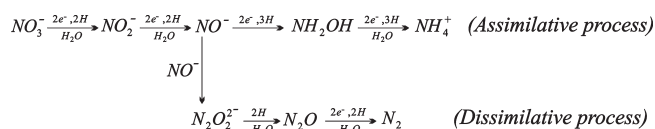
the respective k_1 and k_{II} values obtained by Gao et al.⁸ for small TiO₂ particles. In the latter study, the fast and slow decay rate constants were suggested to correspond to the reaction of stored electrons with the adsorbed H₂O₂ molecules and H₂O₂ molecules in the bulk, respectively.

The number of consumed electrons can also be determined from the kinetic curves shown in Figures 4 and 5 for the case that the initial concentration of the electron acceptor is lower than the initial concentration of the stored electrons. Thereby, it is found that in the presence of molecular oxygen an average of 3.1 electrons are transferred per O₂ molecule, while in the presence of H₂O₂, an average of 1.6 electrons are transferred to each H₂O₂ molecule. Safrany et al.¹³ estimated a similar value of 3.3 electrons consumed during the reduction of one oxygen molecule employing radiation induced TiO₂ electrons. The authors attributed this to the occurrence of two parallel pathways, that is, the two and the four electron reduction of O₂ to water, which can be explained as follows: in acidic medium molecular oxygen reacts with one electron producing HO₂[•] radicals (eq 8), which are known to disproportionate to O₂ and H₂O₂ (eq 9). Thus, oxygen effectively reacts with two electrons to produce H₂O₂. However, no H₂O₂ could be detected here after mixing suspensions of stored $e^-_{\text{TiO}_2}$ with acidic aqueous solutions containing O₂ using a sensitive enzymatic analytical method.¹⁵ Presumably, H₂O₂ remains on the TiO₂ surface where it rapidly reacts with another electron producing an [•]OH radical and a OH⁻ ion (eq 10), which is neutralized in acidic solution (eq 11). The [•]OH radical reacts with methanol by hydrogen abstraction resulting in the formation of a [•]CH₂OH radical (eq 12), which can in turn transfer an electron to TiO₂ (eq 13). This pathway results in the reduction of one oxygen molecule to water consuming a net amount of only two electrons. On the other hand, when hydrogen peroxide reacts with two electrons (eq 14), the reduction of oxygen to water requires a net amount of four electrons.

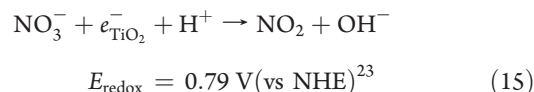


2. Reaction of $e^-_{\text{TiO}_2}$ with Nitrate Ions. The photocatalytic reduction of nitrate has recently received special attention in view of pollution control.^{16–21} Therefore, it is of particular interest to study the kinetics of these reduction reactions by the stored TiO₂ electrons.

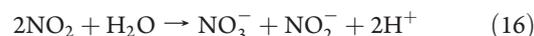
There are two ways of reducing nitrate and nitrite ions, that is, the dissimilative and the assimilative process, yielding N₂ gas and ammonia, respectively.²²



According to the scheme above, five or eight electrons are required to reduce nitrate to N₂ or ammonia, respectively. Moreover, also the one-electron reduction of nitrate ions is feasible in photocatalytic systems:



In aqueous solutions, NO₂ will, however, disproportionate according to the following equation:



Thus, eqs 15 and 16 cannot be easily distinguished from the two electron reduction of nitrate forming nitrite.

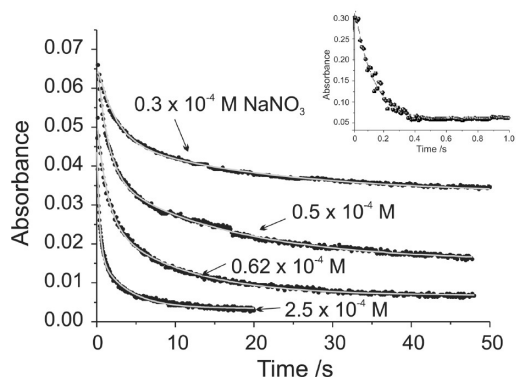
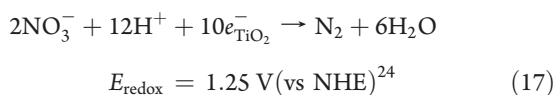
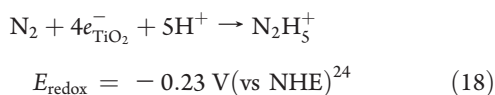


Figure 6. Time profiles of the decay of $e^-_{\text{TiO}_2}$ absorbance at 600 nm ($[e^-_{\text{TiO}_2}] = 5.5 \times 10^{-4}$ M) upon mixing with deaerated (argon purged) aqueous NaNO_3 solutions at pH 2.3, solid lines show the double exponential fits. Inset shows time profile of the decay of $e^-_{\text{TiO}_2}$ absorbance at 600 nm ($[e^-_{\text{TiO}_2}] = 2.5 \times 10^{-3}$ M) upon mixing with N_2 saturated aqueous solutions at pH 2.3.

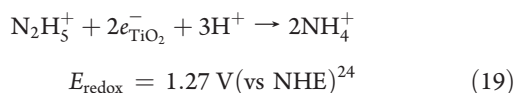
In the presence of excess electrons two nitrate ions can rather react by a 10 electron transfer step to form N_2 via



N_2 in turn can react by a four electron transfer reaction to produce N_2H_5^+ ions



N_2H_5^+ will further react with two electrons to produce 2NH_4^+ ions



In the present kinetic study, stopped flow experiments were performed by mixing the stored electrons in TiO_2 and aqueous nitrate solution at acidic pH (2.3).

The transient decays of the absorbance of the TiO_2 electrons ($[e^-_{\text{TiO}_2}] = 5.5 \times 10^{-4}$ M) upon mixing with various concentrations of sodium nitrate in aqueous solution are shown in Figure 6. The kinetic curves were analyzed according to double exponential decays (cf. solid lines in Figure 6). The observed first order rate constants of both decay processes are found to increase linearly with increasing nitrate ion concentrations. The respective second order rate constants were obtained from the slope of the linear dependencies and are summarized in Table 1. The values of the second order rate constants obtained here differ considerably from those reported by Gao et al.⁸ This is readily explained by the fact that these authors observed the one electron reduction of nitrate ions while in the present study a multi-electron transfer is occurring (the concentration of electrons employed in their experiments are considerably lower than the electron concentration employed here).

It is in fact estimated that an overall of about 8 electrons are consumed per NO_3^- ion which is in consistence with the

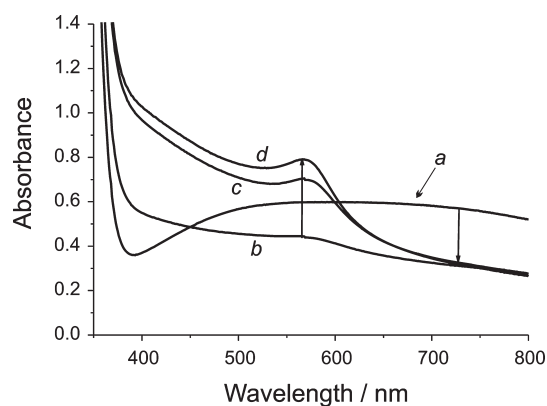


Figure 7. Steady state UV-vis measurements, while Cu^0 nanoparticles grow as indicated from the surface plasmon absorbance with maximum at 570 nm after bringing in contact TiO_2 electrons ($[e^-_{\text{TiO}_2}] = 5.5 \times 10^{-4}$ M) with a Cu^{2+} solution ($[\text{Cu}^{2+}] = 2.5 \times 10^{-4}$ M) (a) stored TiO_2 electrons before mixing (b) immediately after mixing, (c) after 2 min and (d) after 4 min of mixing with the Cu^{2+} solution.

stoichiometry of the assimilative pathway of reduction of nitrate ions to ammonia.

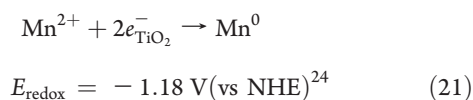
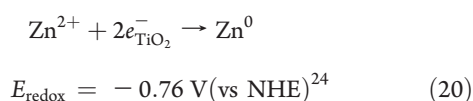
According to the observed results and the estimated number of electrons for each decay step (see Table 1), the mechanism can be described as follows: in the presence of excess electrons initially a five electron transfer process occurs leading to the reduction of nitrate to N_2 (eq 17), the latter can be further reduced to ammonia through eqs 18 and 19. To confirm the reaction of N_2 gas with excess $e^-_{\text{TiO}_2}$, a stopped flow experiment was performed mixing an aqueous TiO_2 electron suspension (2.5×10^{-3} M $e^-_{\text{TiO}_2}$) with a N_2 saturated aqueous solution ($[\text{N}_2]_{\text{aq}} = 3.35 \times 10^{-4}$ M)²⁵ at pH 2.3. The $e^-_{\text{TiO}_2}$ absorbance decays according to a first order rate law (cf. inset of Figure 6). From the resulting first order rate constant of 5.9 s^{-1} a second order rate constant $k_2 = 1.8 \times 10^4 \text{ M}^{-1} \text{ s}^{-1}$ is calculated. This rate constant is faster than that obtained for the slow process in the reduction of nitrate which is expected to be due to the reduction of molecular nitrogen to ammonia (eqs 18 and 19). This can be readily understood as the steady state concentration of N_2 gas that is reduced during the reduction of nitrate ions which will be much lower than the N_2 concentration employed in the experiment of $e^-_{\text{TiO}_2}$ and molecular nitrogen ($e^-_{\text{TiO}_2} + \text{N}_2$).

It is calculated that ~ 6 electrons were consumed per N_2 molecule in agreement with the theoretical number of electrons required for the reduction of N_2 gas to ammonia.

The formation of ammonia was furthermore confirmed by performing separate experiments, that is, by the 1:1 mixing of aqueous suspensions of TiO_2 electrons and NaNO_3 solutions (under the conditions identical to those of the kinetic experiments) in an isolated reactor and measuring the evolved ammonia by Nessler's method.²⁶ The pH of the resulting mixed solutions were adjusted to 9 by adding NaOH , then the solutions were cooled to 4°C . Nessler's reagent (0.09 M solution of potassium tetraiodomercurate(II) ($\text{K}_2[\text{HgI}_4]$) in 2.5 M potassium hydroxide) was then added slowly to the cooled solutions. Strong yellow-brown colorations were observed indicating the presence of ammonia. In addition, GC measurements of the headspace above the mixed solutions indicated the absence of any measurable amounts of N_2 gas.

3. Reaction of $e^-_{\text{TiO}_2}$ with Zn^{2+} and Mn^{2+} . It was observed that after mixing the aqueous suspension of stored TiO_2

electrons (2×10^{-3} M) with an acidic solution containing either Zn^{2+} (0.5×10^{-3} M ZnCl_2) or Mn^{2+} (0.5×10^{-3} M MnCl_2), the absorbance signals remain stable even over 200 s, indicating that eqs 20 and 21 did not occur.



This can be attributed to the fact that the values of the redox potentials of Zn^{2+} and Mn^{2+} are considerably more negative than the potential of the stored electrons on the TiO_2 (-0.5 V vs NHE).²⁷

4. Reaction of $e_{\text{TiO}_2}^-$ with Cu^{2+} . Effluents from electroplating, electrical and leather industry, and machinery contain often high concentrations of copper ions. This places Cu^{2+} on the list of strategically important metals. Moreover, environmental pollution caused by copper contamination must not be neglected.²⁸ The detailed understanding of the kinetics and the mechanism of the photocatalytic reduction of Cu^{2+} ions is thus of crucial importance to develop respective systems for the removal of these metal ions from waste streams. It has been reported that Cu^{2+} can be reduced to Cu^0 by TiO_2 electrons.^{29,30} Herrmann et al.³¹ suggested that in the presence of TiO_2 suspensions Cu^{2+} ions are not reduced to Cu^0 but to Cu^+ even in the absence of molecular oxygen. In the present study, aqueous solution of Cu^{2+} ions were mixed with stored TiO_2 electrons and the reaction products were detected by steady state absorption spectroscopy as well as by following the reaction kinetics by stopped flow measurements.

Figure 7 shows the steady state UV-vis spectra recorded immediately and after various times of mixing of TiO_2 electrons and Cu^{2+} ions from CuCl_2 aqueous solution. Because the reduction of Cu^{2+} ions depends strongly on the presence of molecular oxygen, great care was taken to exclude molecular oxygen as far as possible during the manipulation of the solutions. As the broad absorption of TiO_2 electrons decays, the surface plasmon absorption of colloidal copper with a maximum at 570 nm³² develops. The blue suspension of TiO_2 electrons turned to the ruby-red color of colloidal copper after mixing with an aqueous solution of Cu^{2+} ions. A two-electron transfer reaction is thus assumed to take place resulting in the formation of copper atoms (eq 22), which form colloidal copper nanoparticles (eq 23)



It was difficult to determine the size of the deposited copper particles by means of transmission microscopy since the particles were very sensitive toward molecular oxygen and completely dissolved by exposure to air within a few minutes. Moreover, no theoretical correlation between the size of the copper particles and the position of their surface plasmon band could be found in the literature. Hence, the particle size of the Cu_n^0 could not be estimated from the UV-vis spectra (cf. Figure 7).

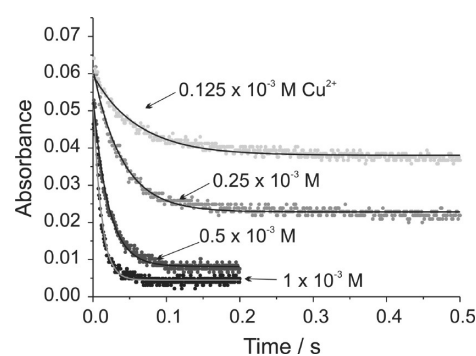


Figure 8. Time profiles of the decay of $e_{\text{TiO}_2}^-$ absorbance at 600 nm ($[e_{\text{TiO}_2}^-] = 5.5 \times 10^{-4}$ M) upon mixing with deaerated (Ar purged) aqueous CuCl_2 solutions of different concentrations at pH 2.3, solid lines show the first order fits.

The kinetics of the reaction between TiO_2 electrons and Cu^{2+} ions were studied by performing stopped flow mixing experiments of TiO_2 electron suspensions with various concentrations of CuCl_2 in aqueous solutions in the absence of oxygen (Figure 8). A first order rate law was observed at all Cu^{2+} concentrations. The second order rate constant obtained from the slope of this linear dependency is $k_2 = 9.4 \times 10^4 \text{ M}^{-1} \text{ s}^{-1}$. This value is very similar to the value obtained by Gao et al.⁸ ($1.3 \pm 0.3 \times 10^5 \text{ M}^{-1} \text{ s}^{-1}$), however, the authors attributed this rate constant to the one electron reduction of Cu^{2+} to Cu^+ .

Following the fast initial decay, a slow build up of a transient absorbance is observed at 570 nm (not shown). The build-up of this signal can be fitted by a first order rate kinetics. The second order rate constant of the TiO_2 electron absorbance decay and the first order rate constant of the Cu^0 particles growth are summarized in Table 1.

It was calculated from the kinetic decays that an average between 1.9 and 1.5 electrons are consumed per Cu^{2+} ion which is lower than the theoretical value of 2 because the absorbance of the products (Cu_n^0) also contribute to the absorbance at the same wavelength where $e_{\text{TiO}_2}^-$ absorb.

CONCLUSIONS

This work focuses on the analysis of the dynamics of multi-electron transfer reactions in photocatalytic systems utilizing the stopped flow technique to study the reactions of stored electrons in TiO_2 nanoparticles with various electron acceptors. The TiO_2 conduction band electrons have been photogenerated on nano-sized TiO_2 particles upon UV (A) illumination in the presence of a hole scavenger (methanol) and stored in the absence of molecular oxygen. The results obtained from this study can be summarized as follows: (1) the stored TiO_2 electrons reduce O_2 and H_2O_2 to water by multi-electron transfer processes; (2) the stored TiO_2 electrons are able to reduce nitrate ions to ammonia through the transfer of eight electrons with the intermediate formation of molecular nitrogen; (3) Cu(II) ions are reduced through a two-electron transfer reaction to form Cu(0) nanoparticles which are detected by their typical surface plasmon resonance band at 570 nm. Neither the reduction of Zn^{2+} nor that of Mn^{2+} can be induced using stored TiO_2 electrons in these systems, attributing it to the thermodynamic infeasibility of the respective reduction processes.

■ AUTHOR INFORMATION

Corresponding Author

*E-mail: bahnmann@iftc.uni-hannover.de.

■ ACKNOWLEDGMENT

H.H.M. gratefully acknowledges the Egyptian Ministry of Higher Education for granting her a doctoral scholarship.

■ REFERENCES

- (1) Hoffmann, M. R.; Martin, S. T.; Choi, W.; Bahnmann, D. W. *Chem. Rev.* **1995**, *95*, 69–96.
- (2) Litter, M. I. *Appl. Catal., B* **1999**, *23*, 89–114.
- (3) Bahnmann, D. W.; Henglein, A.; Lilie, J.; Spanhel, L. *J. Phys. Chem.* **1984**, *88*, 709–711.
- (4) O'Regan, B.; Grätzel, M.; Fitzmaurice, D. *Chem. Phys. Lett.* **1991**, *183*, 89–93.
- (5) Boschloo, G.; Fitzmaurice, D. *J. Phys. Chem. B* **1999**, *103*, 2228–2231.
- (6) Grätzel, M.; Frank, A. J. *J. Phys. Chem.* **1982**, *86*, 2964–2967.
- (7) Bahnmann, D. W.; Hilgendorff, M.; Memming, R. *J. Phys. Chem. B* **1997**, *101*, 4265–4275.
- (8) Gao, R.; Safrany, A.; Rabani, J. *Radiat. Phys. Chem.* **2003**, *67*, 25–39.
- (9) Kormann, C.; Bahnmann, D. W.; Hoffmann, M. R. *J. Phys. Chem.* **1988**, *92*, 5196–5201.
- (10) Rajeshwar, K. *J. Appl. Electrochem.* **1995**, *25*, 1067–1082.
- (11) Serpone, N.; Terzian, R.; Lawless, D.; Kennepohl, P.; Sauve, G. *J. Photochem. Photobiol., A* **1993**, *73*, 11–16.
- (12) Wang, C.; Bahnmann, D. W.; Dohrmann, J. K. *Water Sci. Technol.* **2001**, *44*, 279–286.
- (13) Safrany, A.; Gao, R.; Rabani, J. *J. Phys. Chem. B* **2000**, *104*, 5848–5853.
- (14) Kölle, U.; Moser, J.; Grätzel, M. *Inorg. Chem.* **1985**, *24*, 2253–2258.
- (15) Shiraishi, F.; Nakasako, T.; Hua, Z. *J. Phys. Chem. A* **2003**, *107*, 11072–11081.
- (16) Stanbury, D. M. *Adv. Inorg. Chem.* **1989**, *33*, 69–138.
- (17) Ranjit, K. T.; Viswanathan, B. *J. Photochem. Photobiol., A* **1997**, *108*, 73–78.
- (18) Ranjit, K. T.; Viswanathan, B.; Varadarajan, T. K. *J. Mater. Sci. Lett.* **1996**, *15*, 874–877.
- (19) Ranjit, K. T.; Varadarajan, T. K.; Viswanathan, B. *J. Phys. Chem. A* **1995**, *89*, 67–68.
- (20) Zhang, F.; Pi, Y.; Cui, J.; Yang, Y.; Zhang, X.; Guan, N. *J. Phys. Chem. C* **2007**, *111*, 3756–3761.
- (21) Halmann, M.; Zuckerman, K. *J. Chem. Soc., Chem. Commun.* **1986**, 455–462.
- (22) Vicente, F.; Garcia-Jareno, J. J.; Tamarit, R.; Cervilla, A.; Domenech, A. *Electrochem. Acta* **1995**, *40*, 1121–1126.
- (23) Douglas, B.; McDaniel, D. H.; Alexander, J. J. *Concepts and Model of Inorganic Chemistry*, 2nd ed.; Wiley: New York, 1983.
- (24) (a) Shriver, D. F.; Atkins, P. W.; Langford, C. H. *Inorganic Chemistry*; Oxford University Press: New York, 1990. (b) Bard, A. J.; Parsons, R.; Jordan, J. *Standard Potential in Aqueous Solution*; Dekker: New York, 1985.
- (25) Booth, G.; McDuel, B.; Sears, J. *World of Science*; Oxford University Press: New York, 1999.
- (26) Langea, B.; Vejdělek, Z. *J. Photometrische Analyse*; Verlag Chemie: Weinheim, 1980.
- (27) Grätzel, M. *Nature* **2001**, *414*, 338–344.
- (28) Salomons, W.; Förstner, U.; Mader, P., Eds. *Heavy Metals, Problems and Solutions*; Springer: Berlin, 1995; p 386.
- (29) Reiche, H.; Dunn, W. W.; Bard, A. J. *J. Phys. Chem.* **1979**, *83*, 2248–2251.
- (30) Ward, M. D.; Bard, A. J. *J. Phys. Chem.* **1982**, *86*, 3599–3805.

(31) Herrmann, J.-M.; Disdier, J.; Pichat, P. *J. Phys. Chem.* **1986**, *90*, 6028–6034.

(32) Henglein, A. *J. Phys. Chem. B* **2000**, *104*, 1206–1211.

(33) Nadtochenko, V.; Kiwi, J. *Inorg. Chem.* **1998**, *37*, 5233–5238.